

Measuring single-cell density

William H. Grover^{a,b,1}, Andrea K. Bryan^{a,b,1}, Monica Diez-Silva^c, Subra Suresh^{b,c,d,e}, John M. Higgins^{f,g,h}, and Scott R. Manalis^{a,b,d,2}

^aKoch Institute for Integrative Cancer Research, Massachusetts Institute of Technology, Cambridge, MA 02139; ^bDepartment of Biological Engineering, Massachusetts Institute of Technology, Cambridge, MA 02139; ^cDepartment of Materials Science and Engineering, Massachusetts Institute of Technology, Cambridge, MA 02139; ^dDepartment of Mechanical Engineering, Massachusetts Institute of Technology, Cambridge, MA 02139; ^eHarvard–Massachusetts Institute of Technology Division of Health Sciences and Technology, Cambridge, MA 02139; ^fCenter for Systems Biology, Massachusetts General Hospital, Boston, MA 02114; ^gDepartment of Pathology, Massachusetts General Hospital, Boston, MA 02114; and ^hDepartment of Systems Biology, Harvard Medical School, Boston, MA 02115

Edited by David A. Weitz, Harvard University, Cambridge, MA, and approved May 23, 2011 (received for review March 24, 2011)

We have used a microfluidic mass sensor to measure the density of single living cells. By weighing each cell in two fluids of different densities, our technique measures the single-cell mass, volume, and density of approximately 500 cells per hour with a density precision of 0.001 g mL⁻¹. We observe that the intrinsic cell-to-cell variation in density is nearly 100-fold smaller than the mass or volume variation. As a result, we can measure changes in cell density indicative of cellular processes that would be otherwise undetectable by mass or volume measurements. Here, we demonstrate this with four examples: identifying *Plasmodium falciparum* malaria-infected erythrocytes in a culture, distinguishing transfused blood cells from a patient's own blood, identifying irreversibly sickled cells in a sickle cell patient, and identifying leukemia cells in the early stages of responding to a drug treatment. These demonstrations suggest that the ability to measure single-cell density will provide valuable insights into cell state for a wide range of biological processes.

cell size | apoptosis | hematology | biosensor | suspended microchannel resonator

Cells adjust their mass-to-volume ratio during important processes such as cell cycle progression (1), apoptosis (2, 3), differentiation (4), disease state (5, 6), and malignant transformation (7). Although important insights have come from tracking single-cell volume during such processes, and methods for monitoring cell mass are emerging, there currently does not exist a means for measuring the density of individual cells with meaningful precision.

Existing density measurements generally rely on buoyant force to transport cells to a location where the surrounding fluid density most closely equals the cell's density. Even when sped up by centrifugation, lengthy exposure to concentrated solutions of the substance used to construct the density gradient may inadvertently affect the density and viability of the cells. Density gradients also have a fundamental tradeoff between dynamic range and resolution, and construction of a high-resolution but narrow-range density gradient requires that the cell density be known a priori. Combined with the difficulty of tracking single cells in centrifuge tubes, these limitations have precluded the use of density gradient centrifugation for quantifying the density of individual cells. More recently, magnetic levitation has been used to accurately measure the density of micron-scale particles (8), but the concentrated metal salt solutions required are incompatible with living cells.

The ideal method for measuring a single cell's density would not rely on buoyant force to slowly push the cell, but would measure the buoyant force on the cell directly, in any desired fluid, and then use this information to calculate not only the density but also the mass and volume of the cell. Remarkably, such a method was used around 250 B.C. by Archimedes of Syracuse, who was asked by the king to determine whether a crown was made of pure gold. One version of this story suggests that Archimedes measured the density of the crown by hanging it in

a fluid and using a balance to measure the submerged crown's buoyant mass m_b :

$$m_b = m \left(1 - \frac{\rho_f}{\rho} \right),$$

where m is the mass of the crown, ρ_f is the density of the fluid, and ρ is the density of the crown. By measuring the buoyant mass of the crown in two fluids of different known densities (for example, water and air), Archimedes could then calculate the density of the crown and compare it to the known density of pure gold (Fig. 1).

We have implemented Archimedes' method in a microfluidic system to measure the density of single cells. This approach requires both a system to weigh single cells with femtogram precision and a method to rapidly exchange the fluid surrounding a single cell during laminar flow. The "balance" we use to weigh cells in two different fluids is the suspended microchannel resonator (SMR), a microfabricated microfluidic mass sensor (9). As shown in Fig. 2, the SMR consists of a silicon cantilever containing an embedded microfluidic channel. The cantilever oscillates at a frequency that is proportional to its mass, and a cell passing through the embedded channel changes the resonance frequency of the cantilever by an amount proportional to the buoyant mass of the cell. Previous work with the SMR showed that the average density of a population of cells can be calculated from buoyant mass measurements (10, 11) and that yeast exhibit cell cycle-dependent variations in average cell density (11), but these methods cannot measure the density of single cells or derive statistics about the density distribution.

To measure single-cell density with the SMR, the device is first loaded with two different fluids: one containing the cells of interest in any buffer or media (red in Fig. 2), and another with the same tonicity as the first solution but greater density (blue in Fig. 2). The density of the red fluid is determined from the resonance frequency of the cantilever while filled with red fluid (Fig. 2, step 1). A cell's buoyant mass in the red fluid is then recorded from the height of the peak in the resonance frequency while the cell passes through the cantilever (Fig. 2, step 2). The cell then enters the blue fluid, where the faster flow rate quickly dilutes and replaces the red fluid surrounding the cell. Replacing most of the fluid around the cell occurs in as little as 1 s, a

Author contributions: W.H.G., A.K.B., M.D.-S., S.S., J.M.H., and S.R.M. designed research; W.H.G., A.K.B., M.D.-S., and J.M.H. performed research; W.H.G., A.K.B., M.D.-S., S.S., J.M.H., and S.R.M. analyzed data; and W.H.G., A.K.B., M.D.-S., S.S., J.M.H., and S.R.M. wrote the paper.

Conflict of interest statement: S.R.M. is a cofounder of Affinity Biosensors and declares competing financial interests.

This article is a PNAS Direct Submission.

¹W.H.G. and A.K.B. contributed equally to this work.

²To whom correspondence should be addressed. E-mail: scottm@media.mit.edu.

This article contains supporting information online at www.pnas.org/lookup/suppl/doi:10.1073/pnas.1104651108/-DCSupplemental.

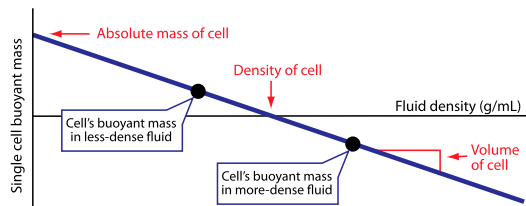


Fig. 1. Applying Archimedes' method to measure single-cell mass, volume, and density. By weighing a cell in two fluids of different density and plotting the linear relationship between buoyant mass and fluid density, the absolute mass, volume, and density of the cell can be determined from the y intercept, slope, and x intercept, respectively.

remarkably fast exchange for a free-flowing cell in laminar flow conditions. The direction of flow is then reversed, blue fluid fills the cantilever (Fig. 2, step 3), and the cell passes through the cantilever a second time to measure its buoyant mass in the blue fluid (Fig. 2, step 4). Sample raw resonance frequency data from the measurement of 12 human erythrocytes in 1 min is shown in Fig. 3. The cell spends very little time (as little as 3 s) in contact with the high-density blue fluid before its buoyant mass is measured. From these two measurements of buoyant mass, the absolute mass, volume, and density of the cell can be calculated (Fig. 1). This process takes approximately 5 s per cell, and the system can measure approximately 500 cells per hour.

Results and Discussion

To validate our method, we measured beads with known density and size. Fig. 4A shows the bead volume, mass, and density distributions for a sample of 5.0- μm -diameter polystyrene beads. The coefficient of variation (CV) of bead density is almost thirty times smaller than the CV of bead volume or mass. The error bars on the plot of bead mass vs. density (Fig. 4B) provide an upper estimate of the resolution of our method: 3 pg absolute mass, 3 fL volume, and 0.001 g mL^{-1} density (\pm one standard deviation). To validate our method using a cell sample, we measured *Plasmodium falciparum* malaria-infected erythrocytes (Fig. 4C). *P. falciparum* is known to cause significant physical changes in infected erythrocytes (5, 12). The observed fraction of low-density infected cells is consistent with earlier studies (5); these infected cells cannot be distinguished from healthy cells by mass, but are clearly distinguishable by density.

In a small-scale blood study, we measured single-cell volume, mass, and density for approximately 500 human erythrocytes from each of 16 patients. Hemoglobin concentration and erythrocyte volume are well known to be altered in various diseases (13). Because hemoglobin comprises about one-third of the mass of an

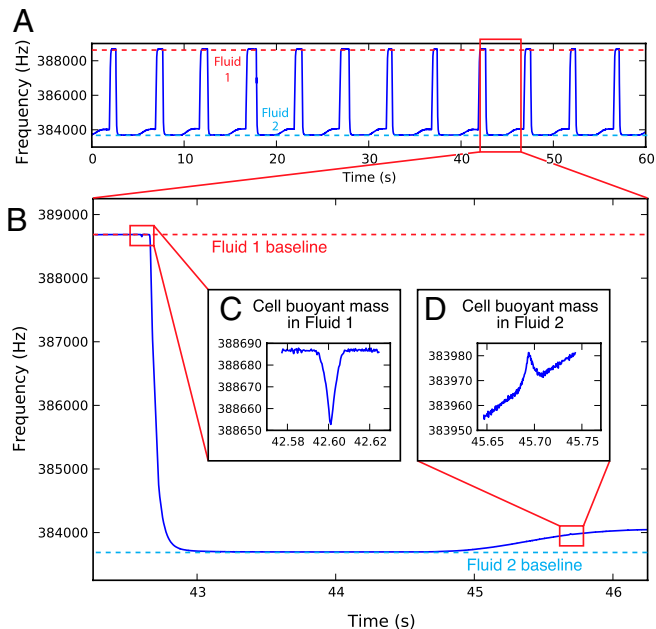


Fig. 3. (A) One minute of the raw resonance frequency of the SMR for 12 cell density measurements. On this scale, only the fluctuations caused by the switching between two different buffer densities are visible. (B) Close-up of the measurement of a single healthy human erythrocyte, showing (C) an approximately 30-Hz downward peak in the SMR resonance frequency as the cell surrounded by Fluid 1 is measured, then a large (approximately 5,000-Hz) decrease as more-dense Fluid 2 passes through the cantilever, and finally (D) an approximately 10-Hz upward peak as the cell surrounded by Fluid 2 is measured. A small amount of Fluid 1 enters the Fluid 2 stream during the first pass of the cell through the cantilever (C); some of this dilute mixture accompanies the cell during its second pass through the cantilever and causes a gradually increasing baseline around the second peak (D).

erythrocyte, we hypothesized that erythrocyte density may also correlate with different cell states. In addition, nine of these individuals received recent blood transfusions prior to analysis. By analyzing blood from transfusion recipients, we explored whether the combination of single-cell volume, mass, and density could be used to distinguish host and donor erythrocytes. This ability could then be used to assess the survival of transfused cells (14) or possibly identify athletes who have received performance-enhancing transfusions (“blood doping”).

Fig. 4D and E show plots of erythrocyte mass vs. density for two transfusion recipients. The sample in Fig. 4D (red points) is from an individual suspected to have thalassemia trait, a genetic

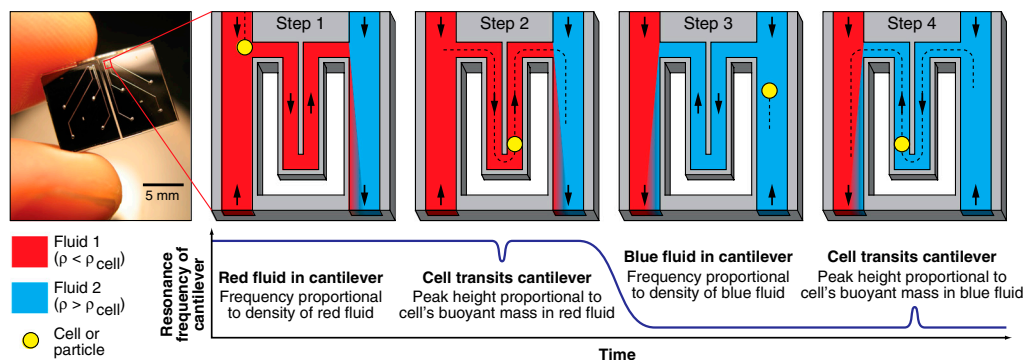


Fig. 2. Using the SMR (Left) to measure the buoyant mass of a cell in two fluids of different densities. Measurement starts with the cantilever filled with any buffer or media less dense than the cell (red, step 1). The density of the red fluid is determined from the baseline resonance frequency of the cantilever. When a cell passes through the cantilever (step 2), the buoyant mass of the cell in the red fluid is calculated from the height of the peak in the resonance frequency. The direction of fluid flow is then reversed, and the resonance frequency of the cantilever drops as the cantilever fills with a fluid more dense than the cell (blue, step 3). The buoyant mass of the cell in the blue fluid is measured as the cell transits the cantilever a second time (step 4). From these four measurements of fluid density and cell buoyant mass, the absolute mass, volume, and density of the cell are calculated.

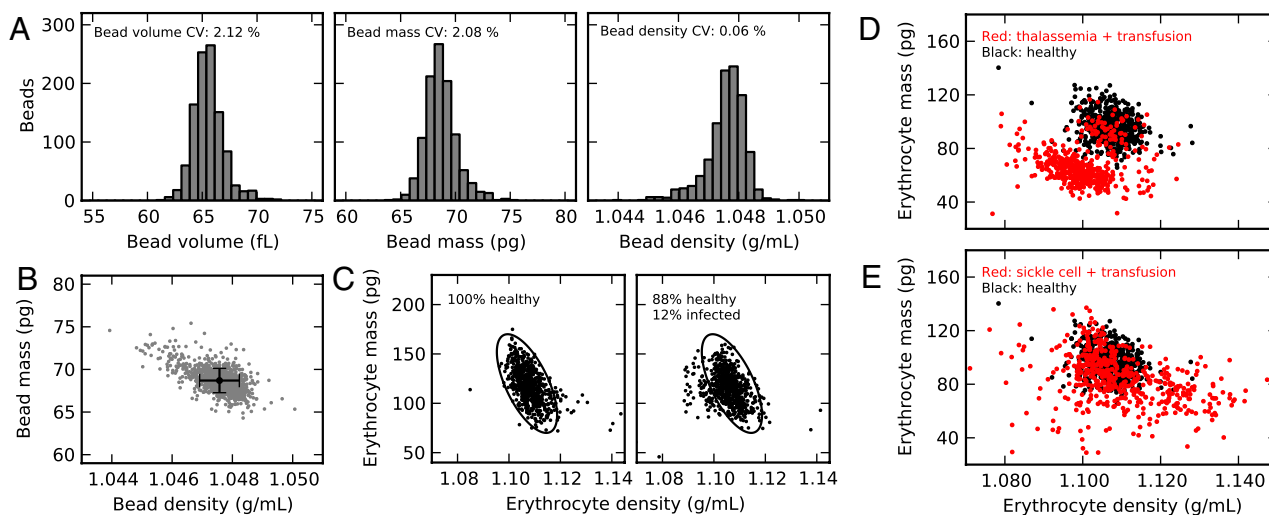


Fig. 4. (A) Bead mass, volume, and density distributions for a population of 5.0- μ m-diameter polystyrene beads ($n = 1,069$), and (B) a scatter plot of bead mass vs. density. Error bars are \pm one standard deviation of the mean. (C) Erythrocyte mass vs. density for 690 cells from a healthy erythrocyte culture (Left) and an equal number of cells from a culture containing approximately 12% *P. falciparum*-infected erythrocytes (Right). The small fraction of less-dense infected cells lies to the left of the healthy cells (circled); these infected cells are indistinguishable by mass but clearly distinguished by density. In this and subsequent plots, the markers are roughly equal in size to the error bars in (B). (D) Single erythrocyte mass vs. density for an individual with suspected thalassemia trait who also received a transfusion of normal (nonthalassemic) blood 4 d prior to collection (red; $n = 502$ cells) compared to a random nonthalassemic, nontransfused individual (black; $n = 502$ cells). The patient's own erythrocytes (red) are offset from a normal patient's erythrocytes (black), except for a small number of normal erythrocytes the thalassemic patient received during the transfusion (red points clustered on black points). (E) Erythrocytes from an individual with sickle-cell anemia who also received a blood transfusion 35 d before collection (red; $n = 502$ cells) compared to the same nontransfused individual as in D (black; $n = 502$ cells). The widening of the distribution of erythrocyte densities in sickle cell anemia is consistent with other studies (6), with the more-dense cells likely representing irreversibly sickled cells (15).

condition that is associated with smaller erythrocyte volumes. Our measurements confirm this and also show smaller erythrocyte masses and densities compared to a random nonthalassemic, nontransfused patient (black points). In addition, a small fraction of normal-mass, normal-density erythrocytes in the thalassemic individual's blood is evident and corresponds to the healthy cells the patient received via transfusion 4 d prior to collection. This diagonally offset subpopulation could only be detected in a multiparameter measurement as demonstrated, and not by isolated measurements of mass, volume, or density. The sample in Fig. 4E (red points) is from a patient with sickle cell anemia who received a transfusion of normal blood 35 d before collection. The widened erythrocyte density distribution is in agreement with earlier studies (6), with the region of more-dense cells likely representing irreversibly sickled cells (15). To assess how an individual's single-cell density changes with time, we obtained two additional samples of blood from the thalassemic patient drawn 1 and 2 d later than the sample analyzed in Fig. 4D. The patient's erythrocyte mass, volume, and density distributions remained essentially unchanged over 3 d (Fig. S1). These measurements show that cell density is by far the most tightly regulated aspect of cell size, but meaningful cell-to-cell variation in density exists, and our method can discriminate the small fraction of transfused blood cells that are only approximately 1% more dense than an individual's own blood cells.

The remaining seven transfusion recipients had no obvious preexisting conditions, so their blood cells should be more similar to cells received via transfusion. In spite of this, our method was sensitive enough to detect a wider range of erythrocyte densities in seven transfusion recipients, compared to seven nontransfused individuals (Fig. S2). These measurements suggest that the density of erythrocytes remain largely unchanged even after the cells have spent days in another individual. We also found that individuals with wider erythrocyte density distributions typically have wider mass and volume distributions as well, though cell density variability is not solely a function of mass or volume variability (Fig. S3). Finally, these 14 individuals' mean erythrocyte densities

do not obviously correlate with the mean cell volume, mean cell hemoglobin content, or hematocrit, as measured by a clinical instrument (Figs. S4 and S5). This suggests that cell density is not merely a function of cellular environment or the concentration of certain cellular components, and that cell density (and the distribution of densities in a population of cells) may be an independent and useful diagnostic.

The observed narrow distribution of density compared to either mass or volume suggests that density could be a unique indicator of changes in cell state that result from environmental perturbations. To test this hypothesis with a model system, we measured mouse lymphocytic leukemia cells (L1210) before and after treatment with staurosporine (STS). STS is a general kinase inhibitor that induces the intrinsic apoptosis pathway and rapidly decreases average cell volume (16–18). Using our method, we observed an approximately 25% decrease in the average cell volume and mass after 20 min of STS treatment (Fig. 5). However, the large cell-to-cell variability in volume and mass would make it impossible to identify treated cells within a background of untreated cells because nearly all treated cells are within the untreated population's distribution (Fig. 5, shaded areas). We observed a much smaller change in average density (approximately 1% increase), yet most treated cells have a density significantly above that of the untreated population's density distribution, thereby demonstrating that only density provides a unique identification of cell state. Interestingly, the rapid and widespread increase in cell density suggests that the cells initially decrease water content rather than increase biomass because biomass synthesis requires longer timescales to affect density significantly. Cells treated with an equal volume of dimethyl sulfoxide (DMSO; control) did not exhibit a change in density, and the 2 μ M concentration of STS does not contribute significantly to the solution osmolarity (>300 mOsm). These early cell density changes may be indicative of constant cell biomass during apoptotic volume decrease, which has not yet been described, or apoptosis-unrelated effects of STS. Nevertheless, the measurement further demonstrates density as an important parameter

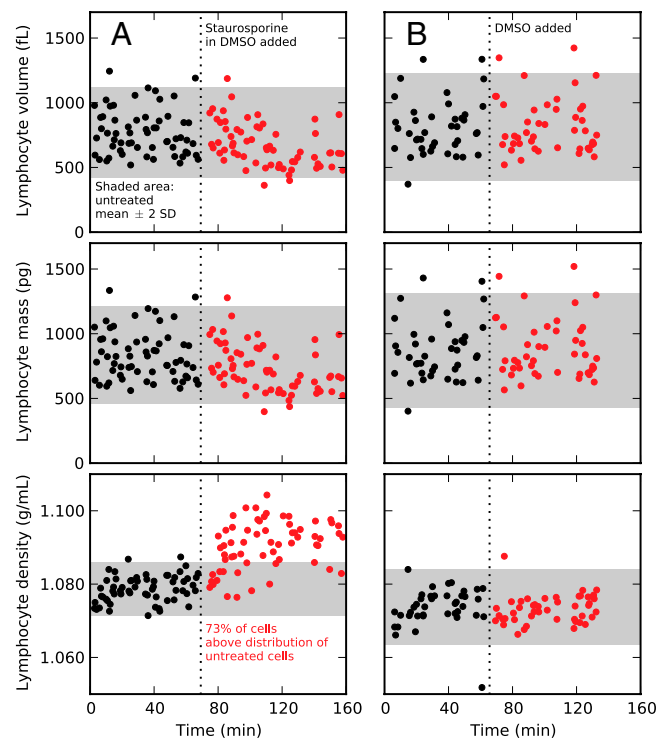


Fig. 5. Time-course data of single-cell masses, volumes, and densities of L1210 mouse lymphocytic leukemia cells before (black) and after (red) the addition of either STS (A; $n = 123$ cells) or an equal volume of DMSO (B; $n = 86$ mock-treated cells). Shaded areas represent the mass, volume, and density distributions of the untreated cells (mean \pm two standard deviations). We observed 73% of treated cells have a density greater than the untreated cells, but <5% of treated cells have a significantly altered mass or volume. Density uniquely identifies the drug-treated cells with a certainty that is impossible by mass or volume measurements.

in distinguishing cell state and our method's ability to measure the properties of large cells (>200 fL) with high precision at the single-cell level.

We have combined a tool for weighing single cells with micro-scale fluid manipulation to develop a rapid and simultaneous measurement of the density, mass, and volume of large numbers of single cells. Our method can discriminate the small fraction of transfused blood cells that are only approximately 1% more dense than an individual's own blood cells. Our technique can also detect a change in cell density that is statistically more significant than the well-known change in cell volume accompanying apoptosis. Methods for measuring fundamental biomechanical and biophysical attributes of single cells have consistently provided valuable insights into cell biology (19, 20), and we anticipate that density, a fundamental property of all cells, will similarly prove to be useful for identifying, distinguishing, and studying single cells.

Materials and Methods

Details of Experimental System. A schematic of the experimental system is shown in Fig. S6. The system contains two parallel paths for fluids (colored red and blue in Fig. 2 and Fig. S6). These two fluid paths are connected through the mass-sensitive SMR. By applying a pressure differential across the resonating microchannel, the contents of either fluid path can be sent through the resonating microchannel and into the other fluid path. Downstream of the SMR, a regulated pneumatic vacuum and two computer-controlled solenoid valves direct the flow of fluid through the system.

During a typical experiment, cells are prepared in any buffer or media at a concentration of 1×10^6 to 1×10^8 cells mL⁻¹ and connected to the red fluid path via capillary tubing inserted into the flask (Fig. S6). The blue fluid path is connected to a flask containing approximately 1 mL of an otherwise-identical buffer with a higher density. To avoid inducing osmotic changes in

the cells, the osmolality of the two fluids should be as similar as possible. Solutions of colloidal silica particles coated with polyvinylpyrrolidone ("Percoll," Sigma-Aldrich) have high density (1.130 g mL⁻¹) and low osmolality (<25 mOs kg⁻¹ H₂O); substituting these solutions for water in a buffer or media recipe increases the fluid's density without significantly altering its osmolality.

To load the cells and fluids into the system, the solenoid valves are switched on to apply high (-70 kPa) vacuum to both downstream waste vials. Within 1 min the red path fills with cells in red fluid and the blue path fills with higher-density blue fluid.

To measure cells, the magnitude of the downstream vacuum is first decreased to approximately -20 kPa, and the solenoid valve connected to the red path is then switched off; this slows the flow of cells in the red path, but the flow of higher-density fluid in the blue path continues (Fig. S6A). The difference in pressures between the two fluid paths causes a cell to flow from the red path through the resonating microchannel and into the blue path. The buoyant mass of the cell in red fluid is recorded as a peak in the resonance frequency of the SMR, and the cell enters the higher-density fluid in the high-flow blue path (Fig. S6B). The states of both solenoid valves are then reversed, so that applied vacuum drives high flow in the red path but flow slows in the blue path. This drives the cell, now surrounded by higher-density fluid from the blue path, back through the resonating microchannel and into the red path (Fig. S6C). The buoyant mass of the cell in the high-density fluid is recorded from the peak in the SMR resonance frequency, and the cell re-enters the high-flow red path. At this point the computer program controlling the system waits for 1 s to ensure that the cell has been flushed down the red path (Fig. S6D), then reverses the states of the solenoid valves again in preparation for measuring the next cell (Fig. S6A again). This process takes approximately 5 s per cell. Every 10 min the regulated vacuum magnitude is increased to -70 kPa for 1 min to load fresh cells from the flask into the SMR. The throughput of the system is approximately 500 cells per hour.

Data Processing. The resulting SMR resonance frequency data contains one pair of peaks for each cell measured. The larger resonating microchannels (15- μ m by 20- μ m fluid channel internal dimensions) used to measure the L1210 mammalian lymphocytes (Fig. 5) yield peaks >100 ms wide; these peaks are well resolved and can be analyzed by smoothing the frequency data with a Savitzky-Golay filter and fitting a second-order polynomial to the peak tip and a line to the baseline. The resulting peak height is proportional to the buoyant mass of the cell in the particular media, and the baseline frequency is proportional to the solution density (calibration details below). The smaller 8- μ m by 8- μ m resonating microchannels used to measure the polystyrene beads (Fig. 4A,B), malaria-infected erythrocytes (Fig. 4C), and transfusion recipient erythrocytes (Fig. 4D and E and Figs. S1-S5) yield peaks only approximately 10 ms wide; the tips of these peaks are not resolved well enough to be analyzed in the same way. Instead, each peak is fit to a calculated peak shape based on the work of Dohn et al. (21) The calculated peak shape is a function of the cell's buoyant mass, the solution density, and other terms describing the peak and baseline. By using the Nelder-Mead method to minimize the sum of squared differences between the experimental and calculated peaks, the cell's buoyant mass and the solution density can be determined.

System Calibration. Two calibrations are necessary to measure cell density with the SMR. The first calibration measures the response of the SMR to a known buoyant mass. Beads with a known volume and density are suspended in a fluid of known density and passed through the resonating microchannel. The resulting peaks are analyzed as described above to determine the mass calibration constant. In practice, this constant remains relatively unchanged throughout the life of an SMR device, so it is typically determined only once. The second calibration measures the response of the SMR to fluid with a known density. Two or more solutions with precisely known densities (for example, sodium chloride solutions prepared gravimetrically) are loaded into the resonating microchannel. Fitting the resulting plot of solution density vs. baseline resonance frequency to a polynomial provides a function for converting SMR resonance frequency to solution density. In practice, the lowest-order term of the polynomial (the y intercept) can change significantly over time due to, e.g., accretion of mass on the inside walls of the resonating microchannel. The resulting error directly affects the measured cell density (for example, a y -intercept term that is 1% too high will result in a measured cell density that is 1% too high). For this reason, we regularly perform a quick and simple single-solution density calibration to determine the y intercept.

Polystyrene bead measurements. For the bead measurements (Fig. 4 A and B), 5.0- μm -diameter polystyrene beads (Duke Scientific/Thermo Fisher Scientific) were diluted to a concentration of approximately 1×10^8 beads mL^{-1} in 1 \times phosphate buffered saline (PBS) containing 0.1% polysorbate 20 ("Tween-20," Sigma-Aldrich).

Malaria Culture Measurements. For the malaria culture measurements (Fig. 4C), *Plasmodium falciparum* 3D7A parasites (Malaria Research and Reference Reagent Resource Center, American Type Culture Collection) were cultured in human erythrocytes (Research Blood Components) in RPMI-1640 complete medium as described elsewhere (22). Approximately 1 mL of each culture (late-stage infected and healthy) was diluted into 10 mL of a simplified RPMI-1640 media (prepared by dissolving 10.44 g RPMI-1640, 5.44 g HEPES, and 2.00 g NaHCO_3 in water for a final volume of 1.0 L). A small volume of the same media was prepared substituting Percoll for water; this was used as the more-dense fluid in the SMR. The diluted cultures were maintained at 37 °C and stirred gently during approximately 2 h of analysis.

Erythrocyte Measurements. For the transfusion recipient erythrocyte measurements (Fig. 4 D and E and Figs. S1–S5), whole blood was obtained from seven patients who had received transfusions within the previous 7 d and from seven patients who had not. Blood samples were obtained under a research protocol approved by the Partners Healthcare Institutional Review Board. Samples were stored at 4 °C until analysis and were analyzed within 32 h of collection. For each sample, 5 μL of whole blood was diluted into 10 mL of 1 \times PBS. To make the more-dense buffer, 100 μL of 10 \times PBS was combined with 900 μL of high-density Percoll (preparation described below). The diluted blood samples were maintained at 25 °C during analysis. A second capillary tube inserted into the diluted blood sample bubbled a gentle stream of air into the vial and kept the cells in suspension during analysis. In this manner, the single-cell density, mass, and volume of approximately 500 erythrocytes were analyzed in approximately 1 h for each patient.

High-density Percoll was prepared by filling 5-mL syringes with Percoll, capping the syringes, and storing the syringes oriented plunger-up at –20 °C for at least 16 h. The syringes were then allowed to thaw at 4 °C over at least 16 h. A freeze-thaw cycle causes a density gradient to form within a tube of Percoll (23). The bottom approximately 1 mL (the densest fraction) was then dispensed from the syringes and used in the above protocol.

Mouse Lymphoblast Culture Measurements. For the L1210 measurements (Fig. 5), cells were grown at 37 °C in L-15 media (Gibco/Invitrogen) supplemented with 0.4% (wt/vol) glucose, 10% (vol/vol) fetal bovine serum,

100 IU penicillin, and 100 $\mu\text{g}/\text{mL}$ streptomycin. Cells were passaged every 2–3 d to maintain a cell concentration of approximately 50,000 mL^{-1} . For the SMR measurements, cells from culture were spun down, resuspended in fresh prewarmed media at a concentration of approximately 100,000 mL^{-1} , and delivered to the SMR. The more-dense buffer consisted of 45% liquid food coloring, 45% 2 \times L-15 Percoll media (pH 7.2), and 10% L-15 media. L-15 Percoll media is identical to the cell culture media with the exception of 50% Percoll (vol/vol) and the use of powdered (Sigma-Aldrich) rather than liquid L-15 media. After approximately 1 h of measurement, cells were treated with 2 μM STS or an equal volume of DMSO (mock-treated control) and measured for an additional hour. The SMR and sample were maintained at 37 °C. The cell sample was added to a glass sample vial to a final depth of less than 0.5 cm, the same fluid depth used in conventional culture flasks. A centrifuge tube containing approximately 1 mL of alternate-density media was placed inside of the glass sample vial to deliver both fluids using the same pressure.

The larger 15- μm by 20- μm resonating microchannel used to measure the L1210 cells (Fig. 5) was interfaced to cells and media as shown in Fig. S6, but using upstream pressure instead of downstream vacuum to drive fluid flow through the system. Three of the four SMR device ports are maintained with a single pressure regulator, and fine pressure corrections at the start of each experiment are individually made to these ports by changing the fluid vial height. The fourth port alternates between a low and high pneumatic pressure source via a computer-controlled solenoid valve (SMC) that responds to the SMR resonance frequency. Actuation of this valve controls the direction of fluid flow through the SMR. Following each flow reversal, a 400-ms, approximately 10% increase in sample pressure is applied to flush away partially mixed fluid and bring in new cells. Every 4.25 min the tubing is flushed with a high-pressure (approximately 70 kPa) rinse for 45 s, and the sample vial is gently shaken to resuspend the cells. No measured cell stays more than 4.25 min in the microfluidic system.

ACKNOWLEDGMENTS. We thank Prof. Marc Kirschner and Dr. Amit Tzur for the L1210 cells and cell culture expertise, and Dr. Paul Jorgensen for many helpful discussions. Funding was provided by EUREKA (R01GM085457) and a Center for Cell Decision Process Grant (P50GM68762) from the US National Institutes of Health and by an Institute for Collaborative Biotechnologies Grant (W911NF-09-D-0001) from the US Army Research Office. A.K.B. is supported by a Whitaker Health Sciences Graduate Fellowship. M.D.-S. and S.S. are funded by National Institutes of Health Grant R01HL094270. J.M.H. is funded by National Institute of Diabetes and Digestive and Kidney Diseases Grant DK083242.

1. Wolff DA, Pertoft H (1972) Separation of HeLa cells by colloidal silica density gradient centrifugation. I. Separation and partial synchrony of mitotic cells. *J Cell Biol* 55:579–585.
2. Martin SJ, Bradley JG, Cotter TG (1990) HL-60 cells induced to differentiate towards neutrophils subsequently die via apoptosis. *Clin Exp Immunol* 79:448–453.
3. Wyllie AH, Morris RG (1982) Hormone-induced cell death. Purification and properties of thymocytes undergoing apoptosis after glucocorticoid treatment. *Am J Pathol* 109:78–87.
4. Maric D, Maric I, Barker JL (1998) Buoyant density gradient fractionation and flow cytometric analysis of embryonic rat cortical neurons and progenitor cells. *Methods* 16:247–259.
5. Mrema JE, Campbell GH, Miranda R, Jaramillo AL, Rieckmann KH (1979) Concentration and separation of erythrocytes infected with *Plasmodium falciparum* by gradient centrifugation. *Bull World Health Organ* 57:133–138.
6. Rodgers GP, Schechter AN, Noguchi CT (1985) Cell heterogeneity in sickle cell disease: Quantitation of the erythrocyte density profile. *J Lab Clin Med* 106:30–37.
7. Bosslet K, Ruffmann R, Altevogt P, Schirrmacher V (1981) A rapid method for the isolation of metastasizing tumour cells from internal organs with the help of isopycnic density-gradient centrifugation in Percoll. *Br J Cancer* 44:356–362.
8. Mirica KA, Shevkopyas SS, Phillips ST, Gupta M, Whitesides GM (2009) Measuring densities of solids and liquids using magnetic levitation: Fundamentals. *J Am Chem Soc* 131:10049–10058.
9. Burg TP, et al. (2007) Weighing of biomolecules, single cells and single nanoparticles in fluid. *Nature* 446:1066–1069.
10. Godin M, Bryan AK, Burg TP, Babcock K, Manalis SR (2007) Measuring the mass, density, and size of particles and cells using a suspended microchannel resonator. *Appl Phys Lett* 91:123121.
11. Bryan AK, Goranov A, Amon A, Manalis SR (2010) Measurement of mass, density, and volume during the cell cycle of yeast. *Proc Natl Acad Sci USA* 107:999–1004.
12. Mills JP, et al. (2007) Effect of plasmodial RESA protein on deformability of human red blood cells harboring *Plasmodium falciparum*. *Proc Natl Acad Sci USA* 104:9213–9217.
13. Goldman L, Bennett JC, eds. (2000) *Cecil Textbook of Medicine* (WB. Saunders, Philadelphia).
14. Steiner ME, et al. (2010) Addressing the question of the effect of RBC storage on clinical outcomes: The Red Cell Storage Duration Study (RECESS). *Transfus Apher Sci* 43:107–116.
15. Bertles JF, Milner PF (1968) Irreversibly sickled erythrocytes: A consequence of the heterogeneous distribution of hemoglobin types in sickle-cell anemia. *J Clin Invest* 47:1731–1741.
16. Ernest NJ, Habela CW, Sontheimer H (2008) Cytoplasmic condensation is both necessary and sufficient to induce apoptotic cell death. *J Cell Sci* 121:290–297.
17. Bortner CD, Cidlowski JA (2004) The role of apoptotic volume decrease and ionic homeostasis in the activation and repression of apoptosis. *Pflügers Arch* 448:313–318.
18. Maeno E, Ishizaki Y, Kanaseki T, Hazama A, Okada Y (2000) Normotonic cell shrinkage because of disordered volume regulation is an early prerequisite to apoptosis. *Proc Natl Acad Sci USA* 97:9487–9492.
19. Suresh S, et al. (2005) Connections between single-cell biomechanics and human disease states: Gastrointestinal cancer and malaria. *Acta Biomater* 1:15–30.
20. Suresh S (2007) Biomechanics and biophysics of cancer cells. *Acta Biomater* 3:413–438.
21. Dohn S, Svendsen W, Boisen A, Hansen O (2007) Mass and position determination of attached particles on cantilever based mass sensors. *Rev Sci Instrum* 78:103303.
22. Trager W, Jensen J (1976) Human malaria parasites in continuous culture. *Science* 193:673–675.
23. Haff LA (1979) Production of Ficoll, Percoll, and albumin gradients by the freeze-thaw method. *Prep Biochem* 9:149–156.